

Localization Leads to Improved Distributed Detection under Non-Smooth Distributions

Nageswara S. V. Rao
Oak Ridge National Laboratory

Jren-Chit Chin, David K. Y. Yau, Chris Y. T. Ma
Purdue University

Abstract – *We consider a detection network of sensors that measure intensity levels due to a source amidst background inside a two-dimensional monitoring area. The source intensity decays away from it possibly in discrete jumps, and the corresponding sensor measurements could be random due to the nature of source and background, or due to sensor errors, or both. The detection problem is to infer the presence of a source based on sensor measurements. In the conventional decision/detection fusion approach, detection decisions are made at the individual sensors using Sequential Probability Ratio Test (SPRT), and are combined at the fusion center using a Boolean fusion rule. We show that better detection can be achieved by utilizing sensor measurements at the fusion center, by first localizing the source and then utilizing a more effective SPRT. This approach leads to the detection performance superior to any Boolean detection fuser, under fairly general conditions: (i) smooth and non-smooth source intensity functions and probability ratios, and (ii) a minimum packing number of the state-space. We apply this method to improve the detection of (a) low-level point radiation sources amidst background radiation under strong shielding conditions, and (b) the well-studied Gaussian source amidst Gaussian background.*

Keywords: Detection network, sequential probability ratio test, cyber physical trade-off, radiation source, detection and localization.

1 Introduction

We consider a network of sensors for detecting a source characterized by a scalar intensity using sensor measurements. The intensity of the source decays away from it and may reach levels comparable to that of background, and in particular the intensity may have discrete drops due to shielding or absorption effects. Sensors measure the intensity at their locations, which may contain random components due to measurement errors, or inherent randomness in the underlying source and background processes (such as radiation), or both.

The prior distribution as well as the intensity and location of the source are not known, but the functional form of sensor measurement distribution is known. The *detection problem* is to infer the presence of such a source based on measurements collected by sensors at known locations. Various formulations of this problem have been studied extensively. The case of Gaussian source amidst Gaussian background process has been studied as a basic problem in distributed detection [22, 26]. In terms of applications, this problem has been studied in the detection of low-level radiation sources particularly in utilizing a network of sensors to achieve performance superior to a single sensor [3, 20].

For single sensors, the detection problem can be solved using a number of well-known methods [21, 22]. The Sequential Probability Ratio Test (SPRT) has been shown to be quite effective, particularly for detecting radiation sources [6, 8, 11]. The SPRT method computes thresholds for the likelihood ratio test to infer the presence or absence of source or insufficiency of measurements to make such decision. When a network of sensors is available, the conventional approach is to utilize SPRT at each sensor and send the Boolean decisions to a fusion center to be combined, for example using a majority or Bayesian fuser. In these solutions, very limited Boolean information is sent from sensors to fusion center, and also the typical fusion rules such as majority require very limited computational resources.

In this paper, we show that by sending the measurements and utilizing a localization method, better detection performance can be achieved under both non-smooth and smooth source intensity and probability ratio functions. Such result was shown first for smooth source profiles and probability ratios in [18], which is not applicable when source intensity is subject to discrete drops. Recently this result has been extended in [14] to non-smooth source mean intensity functions, but it is not applicable when the underlying measurement distributions have discontinuous jumps, as would be the case of radiation sources amidst complex shielding en-

vironments. We present a general result establishing the superiority of localization-based detection, which is valid for a wide-class of smooth and non-smooth source profiles and measurement probability ratios by utilizing a general packing concept of the state-space. In terms of applications, this result encompasses the case of non-isotropic radiation propagation due to shielding effects [10, 2]. This extension requires extending the packing concept used in [18] over finite-dimensional \mathbb{R}^3 to infinite-dimensional functional space as in [14]. Furthermore, we generalize the packing concept of [14] by using a decomposition of the state-space into source parameter space \mathbb{R}^3 and measurements distribution space $\{f : \mathbb{R} \mapsto \mathbb{R}\}$.

This improved performance is achieved by executing a localization algorithm ¹ directly on the sensor measurements at the fusion center, and then using the source estimates in SPRT to infer the presence of source. This result is somewhat counter-intuitive since that localization is generally considered a higher-level function, typically executed after confirming the detection. But, localization computed prior to detection based directly on sensor measurements may lead to “ghost” sources [16]. The main point is that such a ghost source can be ruled-out, thereby confirming a real source, with a higher confidence compared to the detection by a single sensor SPRT (Theorem 3.1) or Boolean fusion of such detections (Theorem 4.1). We apply our results to two cases. First, we consider low-level point radiation sources, whose intensities are of the same order as the background. The measurements in this case are Poisson distributed [10], and hence have high variance, which makes it challenging to distinguish between the source measurements and background noise spikes. Second, we consider the detection of sources that lead to Gaussian distributed measurements [24, 26].

This paper is organized as follows. We formulate the detection problem in Section 2. We present a general result that establishes the relative performance bounds on the detection and false alarm rates of the proposed method compared to fixed-threshold method in Section 3. We compare the performance of the proposed method to majority fuser and a general class of fusers in 4. We discuss the applications of point radiation and Gaussian sources in Section 5.

2 Detection Problem

We consider a two-dimensional monitoring area $\mathcal{M} \subseteq \mathbb{R}^2$, such as $[0, D] \times [0, D]$ -grid, for detecting the presence of a source \mathcal{S} with unknown intensity $A_S \in \mathcal{A}$, $\mathcal{A} = (0, A]$, $A < \infty$ located at an unknown location $(x_S, y_S) \in \mathcal{M}$. The source parameters $(A_S, x_S, y_S) \in \mathbb{R}^+ \times \mathcal{M}$ constitute the *parameter-space* $\mathcal{Z} = \mathcal{A} \times \mathcal{M}$, and are distributed according to $P_{(A_S, x_S, y_S)}$. The

source appears inside \mathcal{M} with a priori probability

$$P_{\mathcal{M}} = \int_{A_S \in \mathcal{A}; (x_S, y_S) \in \mathcal{M}} dP_{(A_S, x_S, y_S)},$$

Both distributions $P_{\mathcal{M}}$ and $P_{(A_S, x_S, y_S)}$ are unknown. There is a background noise process characterized by the intensity parameter $B_{(x,y)} \in \mathcal{B}$, $\mathcal{B} = [0, B]$, $B < \infty$ that depends on the location $(x, y) \in \mathbb{R}^2$, and thus background noise process is parametrized by $P_{(B_{(x,y)}, x, y)}$.

Sensors are located at $M_i = (x_i, y_i) \in \mathbb{R}^2$, $i = 1, 2, \dots, N$ to monitor the area \mathcal{M} ; the sensors may not necessarily be located inside \mathcal{M} . For any point $P = (x, y) \in \mathbb{R}^2$, we have the distance $d(P, M_i) = \sqrt{(x - x_i)^2 + (y - y_i)^2}$, for $1 \leq i \leq N$. For two points in state-space $z_1 = (a_1, x_1, y_1)$, $z_2 = (a_2, x_2, y_2) \in \mathcal{Z}$, we define $d(z_1, z_2) = \sqrt{(a_1 - a_2)^2 + (x_1 - x_2)^2 + (y_1 - y_2)^2}$. The sensor measurements are characterized as follows:

- (a) **Background Measurements:** When there is no source present, the “background” measurements of M_i are distributed according to P_{B_i} , $B_i = B_{(x_i, y_i)}$.
- (b) **Source Measurements:** When the source is present in \mathcal{M} , the intensity at sensor location (x_i, y_i) is A_i which is a function of A_S and $d(S, M_i) = d((x_S, y_S), M_i)$. We represent this dependence explicitly as a function $A_i = F_S(A_S, x_S, y_S, x_i, y_i)$. The measurements of A_i collected at M_i are distributed according to $P_{A_i + B_i}$.

It is assumed that the form of the underlying measurement distributions P_{B_i} and $P_{A_i + B_i}$ are known; for the example for detecting point radiation sources, these distributions are approximated by Poisson process with parameters B_i and $A_i + B_i$, respectively [10, 2, 11]. For the Gaussian source detection problem, these distributions are given by Gaussian distribution with mean parameters B_i and $A_i + B_i$, respectively, and standard deviation σ [26, 24].

Let $m_{i,1}, m_{i,2}, \dots, m_{i,n}$ be the sequence of measurements collected by sensor M_i over an observation time window W , such that $m_{i,t}$, $i = 1, 2, \dots, N$, are collected at the same time t at all sensors.

We consider the *Detection Problem* that deals with inferring the presence of a source inside \mathcal{M} based on measurements collected at M_1, M_2, \dots, M_N . We characterize the solution of the detection problem by the (a) *false alarm probability* $P_{0,1}$, corresponding to the probability of declaring the presence of a source when none exists, and (b) *missed detection probability* $P_{1,0}$, corresponding to the probability of declaring the presence of only the background radiation when a source is present in the monitoring area. The detection probability is given by $P_{1,1} = 1 - P_{1,0}$.

¹Localization is used here as a means to achieve better detection, and is not a requirement to solving the detection problem.

2.1 SPRT Detection

Consider the measurements $m_{i,1}, m_{i,2}, \dots, m_{i,n}$ collected by sensor M_i within a given time window and the background noise level $B_i = B_{(x_i, y_i)}$ at this sensor location. Let H_C , for $C \in \{A_i + B_i, B_i\}$, denote the hypothesis that the measurements correspond to intensity level C at the sensor M_i . Now consider the likelihood function $L(m_{i,1}, m_{i,2}, \dots, m_{i,n} | H_C)$ which represents the probability that the measurements were produced by the source if $C = A_i + B_i$ and just the background if $C = B_i$. The ratio of these likelihood functions can be utilized to decide between these hypotheses. We now consider the following SPRT based on sensor measurements at M_i

$$\mathcal{L}_{A_i, B_i, n} = \frac{L(m_{i,1}, m_{i,2}, \dots, m_{i,n} | H_{A_i+B_i})}{L(m_{i,1}, m_{i,2}, \dots, m_{i,n} | H_{B_i})}$$

which can be used for detecting the source with false positive and missed detection probability parameters $P_{0,1}$ and $P_{1,0}$ respectively as follows [9]:

- (i) If $\mathcal{L}_{A_i, B_i, n} < \frac{P_{0,1}}{1-P_{1,0}}$, then declare the background, namely H_{B_i} ;
- (ii) Else if $\mathcal{L}_{A_i, B_i, n} > \frac{1-P_{0,1}}{P_{1,0}}$, then declare that a source is present, that is $H_{A_i+B_i}$;
- (iii) Otherwise, declare that the measurements are not sufficient to make a decision and continue collecting additional measurements.

The following properties of the SPRT [9] make this test suitable for the present detection problem: (a) The expected false alarm and miss detection rates of SPRT are given by $P_{1,0}$ and $P_{0,1}$, respectively. (b) Among all tests to decide between $H_{A_i+B_i}$ and H_{B_i} with the given $P_{1,0}$ and $P_{0,1}$, SPRT minimizes $E[n | H_{B_i}]$ and $E[n | H_{A_i+B_i}]$ (see Theorem 2.4, [23], for example).

This test can be compactly expressed as

$$\frac{P_{0,1}}{1-P_{1,0}} \leq \mathcal{L}_{A_i, B_i, n} \leq \frac{1-P_{0,1}}{P_{1,0}}$$

Typically, $\mathcal{L}_{A_i, B_i, n}$ cannot be directly applied for our detection problem since it depends on A_i which in turn depends on source location and intensity both of which are unknown. By utilizing the domain knowledge, this test is often expressed in terms of measurements, and we consider such a generic case.

Definition 2.1 We define a likelihood ratio test SPRT to be separable if it can be expressed as

$$\begin{aligned} F_L(P_{0,1}, P_{1,0}, A_i, B_i, n) &< \sum_{j=1}^n m_{i,j} \\ &< F_U(P_{0,1}, P_{1,0}, A_i, B_i, n), \end{aligned}$$

for suitable lower and upper threshold function $F_L(\cdot) \in \mathcal{F}_L$ and $F_U(\cdot) \in \mathcal{F}_U$, respectively.

In practice suitable scalar values τ_L and τ_H are chosen for the upper and lower thresholds respectively, based on domain-specific considerations, Bayesian inference or other method (in addition to choosing appropriate values for $P_{1,0}$ and $P_{0,1}$). We denote the SPRT with such selected threshold by $\mathcal{L}_{\tau_L, \tau_H}$, which will be called *fixed-threshold* SPRT.

2.2 Robust Localization

The *localization* corresponds to estimating the location and strength of the source using measurements $m_{i,j}, i = 1, 2, \dots, N, j = 1, 2, \dots, T$. The estimates of A_S and (x_S, y_S) are denoted by \hat{A}_S and (\hat{x}_S, \hat{y}_S) , respectively. The estimated source parameters will be substituted into the SPRT as follows:

$$\begin{aligned} F_L(P_{0,1}, P_{1,0}, \hat{A}_i, B_i, n) &< \\ \sum_{j=1}^n m_{i,j} &< F_U(P_{0,1}, P_{1,0}, \hat{A}_i, B_i, n) \end{aligned}$$

such that $\hat{A}_i = F(\hat{A}_S, \hat{x}_S, \hat{y}_S, x_i, y_i)$. We denote this SPRT as $\mathcal{L}_{\hat{S}}$, and refer to as the *localization-based* SPRT.

Definition 2.2 A localization method is δ -robust if the following condition can be ensured: there exists $\delta(\epsilon, n, N)$, which is a non-increasing function of number of measurements n and number of sensors N and non-decreasing function of precision ϵ such that

$$P \left\{ (\hat{x}_S, \hat{y}_S, \hat{A}_S) \in \mathfrak{R}_{S, \epsilon} \right\} > \delta(\epsilon, n, N)$$

where $\mathfrak{R}_{S, \epsilon} = \{z \in \mathfrak{R}^3 | d(z, z_S) \leq \epsilon; z_S = (x_S, y_S, A_S)\}$ called ϵ -precision region.

This condition ensures that the estimate is within ϵ of source parameter z_S with probability δ , which improves as more measurements are collected and more sensors are deployed. This condition is a reasonable requirement and is satisfied by algorithms used for localizing point radiation sources under isotropic shielding conditions [17, 17]. However it is much harder to satisfy under arbitrary shielding environments. A general approach in such cases is to execute the localization algorithm on 3-sensor combinations, wherein the sensors are “close-by”. Then results from such localized 3-sensor combinations can be combined to derive the source parameters [17].

3 Improved Detection Through Robust Localization

For a given SPRT \mathcal{L} , we denote the detection and false alarm probabilities by $\mathcal{E}_D(\mathcal{L})$ and $\mathcal{E}_F(\mathcal{L})$, respectively. Let $\mathcal{F} \subseteq \{f : D \mapsto D\}$ denote a class of functions, and $Z \subseteq \mathfrak{R}^3$ denote the set of all possible source parameters. A *spherical cell* with center

$(z_k, f_k) \in Z \times \mathcal{F}$ and radius pair $(\rho_Z, \rho_{\mathcal{F}})$ is defined as

$$\mathcal{C}(z_k, f_k) = \{(z, f) | d_\infty(z, z_k) < \rho_Z; \|f - f_k\|_\infty < \rho_{\mathcal{F}}\},$$

where

$$d_\infty((a_1, a_2, a_3), (b_1, b_2, b_3)) = \max_{i=1,2,3} |a_i - b_i|$$

$$\text{and } \|f - f_k\|_\infty = \max_{x \in D} |f(x) - f_k(x)|.$$

Definition 3.1 A $(\rho_Z, \rho_{\mathcal{F}})$ -packing of state-space $\mathcal{Z} \subseteq Z \times \mathcal{F}$ corresponds to disjoint spherical cells with cell centers at (z_k, f_k) , $k = 1, 2, \dots, K$ of radius pair $(\rho_Z, \rho_{\mathcal{F}})$ all contained inside state-space \mathcal{Z} . We define such a packing to be translation invariant if all cells are still inside \mathcal{Z} when centers are translated as $z + z_k$, for all $z \in \mathcal{Z}$. The state packing number $\mathcal{M}_\infty(\mathcal{Z}, \rho_Z, \rho_{\mathcal{F}})$ denotes the maximum size of translation invariant $(\rho_Z, \rho_{\mathcal{F}})$ -packing of state-space \mathcal{Z} .

We characterize the state-space by the following two parts:

$$\mathcal{Z}_L = Z \times \mathcal{F}_L = \mathcal{A} \times \mathcal{M} \times \mathcal{F}_L, \quad \text{and}$$

$$\mathcal{Z}_H = Z \times \mathcal{F}_H = \mathcal{A} \times \mathcal{M} \times \mathcal{F}_H.$$

Based on measurements at sensor located at (x_i, y_i) , we define two sets that represent all possible source parameters and SPRT bound functions that correspond to the thresholds of $\mathcal{L}_{\tau_L, \tau_H}$ as follows:

$$\begin{aligned} \mathcal{S}_{\tau_L} = \{ & (x_S, y_S, A_S, F_L) \in \mathcal{Z}_L \\ & | \tau_L = F_L(P_{0,1}, P_{1,0}, A_i, B_i, n); \\ & A_i = F_S(A_S, x_S, y_S, x_i, y_i) \} \quad \text{and} \end{aligned}$$

$$\begin{aligned} \mathcal{S}_{\tau_H} = \{ & (x_S, y_S, A_S, F_H) \in \mathcal{Z}_H \\ & | \tau_H = F_H(P_{0,1}, P_{1,0}, A_i, B_i, n); \\ & A_i = F_S(A_S, x_S, y_S, x_i, y_i) \}. \end{aligned}$$

The following theorem presents a general result on the relative performance of the threshold-based SPRT $\mathcal{L}_{\tau_L, \tau_H}$ and localization-based SPRT $\mathcal{L}_{\hat{S}}$. In particular, this theorem specifies a sufficiency condition under which the latter performs better than SPRT implemented based on measurements from single sensor located at (x_i, y_i) . Note that the threshold-based SPRT can be computed at any sensor, whereas the localization-based SPRT requires a network of at least 3 sensors. In this sense, this result captures the conditions under which a network of sensors can be shown to outperform any single sensor within SPRT framework.

Theorem 3.1 Consider the detection of a source under separable SPRT condition. Then for SPRT $\mathcal{L}_{\hat{S}}$ based on δ -robust localization method and any threshold-based SPRT $\mathcal{L}_{\tau_L, \tau_H}$ using measurements from sensor located at (x_i, y_i) , for sufficiently large n and N :

(i) detection rates satisfy

$$\mathcal{E}_D(\mathcal{L}_{\hat{S}}) > [\mathcal{E}_D(\mathcal{L}_{\tau_L, \tau_H}) + (\mathcal{M}_\infty(\mathcal{Z}_L, \epsilon_{D_Z}, \epsilon_{D_{\mathcal{F}}}) - 1)] \delta(\epsilon_{D_Z}, n, N)$$

$$\text{where } \epsilon_{D_Z} = \max_{(z_1, f_1), (z_2, f_2) \in \mathcal{S}_{\tau_H}} d_\infty(z_1, z_2) \quad \text{and}$$

$$\epsilon_{D_{\mathcal{F}}} = \max_{(z, f_1), (z, f_2) \in \mathcal{S}_{\tau_H}} \|f_1 - f_2\|_\infty;$$

(ii) false alarm rates satisfy

$$\mathcal{E}_F(\mathcal{L}_{\hat{S}}) < [\mathcal{E}_F(\mathcal{L}_{\tau_L, \tau_H}) - (\mathcal{M}_\infty(\mathcal{Z}_H, \epsilon_{F_Z}, \epsilon_{F_{\mathcal{F}}}) - 1)] \delta(\epsilon_{F_Z}, n, N)$$

$$\text{where } \epsilon_{F_Z} = \max_{(z_1, f_1), (z_2, f_2) \in \mathcal{S}_{\tau_L}} d_\infty(z_1, z_2) \quad \text{and}$$

$$\epsilon_{F_{\mathcal{F}}} = \max_{(z, f_1), (z, f_2) \in \mathcal{S}_{\tau_L}} \|f_1 - f_2\|_\infty.$$

Proof: The proof outline is similar in Parts (i) and (ii): we compute a spherical cell for $\mathcal{L}_{\tau_L, \tau_H}$ of the state-space in which it does not make an error and compute its diameter to derive the underlying $(\epsilon_Z, \epsilon_{\mathcal{F}})$ values, $(\epsilon_{D_Z}, \epsilon_{D_{\mathcal{F}}})$ for detection rate and $(\epsilon_{F_Z}, \epsilon_{F_{\mathcal{F}}})$ for false alarm rate, for the localization algorithm. Then we utilize ϵ_Z value computed from these diameters for the $\mathcal{L}_{\hat{S}}$ and exploit the monotonicity of δ in n and N to ensure that \hat{S} is within ϵ_Z -precision region. Then we compute the $(\epsilon_Z, \epsilon_{\mathcal{F}})$ -packing of the state-space and identify the cell corresponding to $\mathcal{L}_{\tau_L, \tau_H}$ in which it makes the correct decision. In all other cells $\mathcal{L}_{\hat{S}}$ does not make an error with probability δ and hence offers better performance than the former.

We now provide the details of the bound on the detection rate in Part (i), which assumes that the source is present. Let \mathcal{S}_{τ_H} denote the centroid of \mathcal{S}_{τ_H} and let \mathcal{C}_{τ_H} denote the spherical cell of radius $(\epsilon_{D_Z}, \epsilon_{D_{\mathcal{F}}})$ centered at it. Now consider a $(\epsilon_{D_Z}, \epsilon_{D_{\mathcal{F}}})$ -packing of the state-space (translated if needed) such that one of its spherical cells \mathcal{C}_{τ_H} aligns exactly with \mathcal{S}_{τ_H} . For fixed τ_L and τ_H , $\mathcal{L}_{\tau_L, \tau_H}$ does not make an error if the source lies inside \mathcal{C}_{τ_H} , more precisely, if the source parameters $(x_S, y_S, A_S) \in \{z | (z, f) \in \mathcal{C}_{\tau_H}\}$. But \mathcal{S}_{τ_H} will make an error everywhere else, in particular on all the other spherical cells of $(\epsilon_Z, \epsilon_{\mathcal{F}})$ -packing of the state-space. There are at least $\mathcal{M}_\infty(\mathcal{Z}, \epsilon_{D_Z}, \epsilon_{D_{\mathcal{F}}})$ spherical cells inside state-space, and only one corresponds to \mathcal{S}_{τ_H} over which it does not make an error. On the other hand, $\mathcal{L}_{\hat{S}}$ does not make an error on any of the spherical cell but with probability δ . Thus the detection probability of $\mathcal{L}_{\hat{S}}$ corresponding to these spherical cells is at least $[(\mathcal{M}_\infty(\mathcal{Z}, \epsilon_{D_Z}, \epsilon_{D_{\mathcal{F}}}) - 1)] \delta(\epsilon_{D_Z}, n, N)$. For the spherical cell \mathcal{C}_{τ_H} , however, detection by $\mathcal{L}_{\tau_L, \tau_H}$ is with probability 1 and that by $\mathcal{L}_{\hat{S}}$ is with probability δ , which leads to the inequality in Part (i). \square

The performance, in terms of both \mathcal{E}_D and \mathcal{E}_F , of $\mathcal{L}_{\hat{\mathcal{S}}}$ is better than $\mathcal{L}_{\tau_L, \tau_H}$ by the factor proportional to the packing number $\mathcal{M}_{\infty}(\cdot)$ and $\delta(\cdot)$ with appropriate parameters. Informally speaking, “larger” state-space will have larger packing number, and hence $\mathcal{L}_{\hat{\mathcal{S}}}$ will lead to a more effective detection. In particular, performance of $\mathcal{L}_{\hat{\mathcal{S}}}$ will be increasingly better as one considers larger parameter space \mathcal{Z} , larger functional spaces of SPRT bound functions \mathcal{F}_L and \mathcal{F}_U , more sensors N , and more measurements n . The performance inequalities of Theorem 3.1 are valid no matter how thresholds are chosen for $\mathcal{L}_{\tau_L, \tau_H}$; for example, they can be based on domain-specific knowledge as in radiation source detection, Bayesian inference, or Dempster-Shafer theory.

Theorem 3.1 is a generalization of results in [18, 14] in terms of relaxing the smoothness conditions. In particular, it imposes no smoothness conditions on the source profile function $A_i = F_S(A_S, x_S, y_S, x_i, y_i)$, and measurement distributions P_{B_i} and $P_{A_i+B_i}$. Its utility depends on the estimates of the packing numbers for \mathcal{Z}_L and \mathcal{Z}_H , which in turn depend on the packing numbers of \mathcal{F}_L and \mathcal{F}_H . If \mathcal{F}_L and \mathcal{F}_H satisfy Lipschitz smoothness properties, the packing numbers can be estimated using the underlying Lipschitz constant [15]. Such packing numbers can also be estimated when \mathcal{F}_L and \mathcal{F}_H do not satisfy smoothness conditions. One of the most general conditions under which such packing numbers can be estimated is the finiteness of scale-sensitive dimension [1]; a special case is that of bounded variation that allows discrete jumps in source intensity profiles and measurement distributions.

4 Comparison to Fusers

When SPRT is executed at each of N sensors with possibly different threshold limits, the individual detection results may be combined at the fusion center using methods such as majority fuser or Bayesian fuser. The majority fuser is denoted by \mathcal{L}_M , which only requires that the decisions at the individual sensors be sent to the fusion center. We now consider a broader class of fusers.

Definition 4.1 *The class of positive fusers, denoted by \mathcal{F}_+ , are such that fuser $F_+ \in \mathcal{F}_+$ declares a detection only if at least one sensor declares the detection.*

This class includes a number of well-known fusers, and some of its members may require complex algorithms. In particular this class includes the classical Bayesian optimal fuser under statistical independence condition [5]. This Bayesian fuser combines the sensor decisions linearly with positive coefficients inversely proportional to error probabilities; for this fuser at least one sensor must conclude a detection for fuser to do so. The communications requirements are still low for this fuser but additional error information would be required to compute the output. However, other fusers belonging

to this class may require the sensor measurements at the fusion center [13]. This class of positive fusers excludes the ones that exploit the cases when the individual SPRTs consistently under-perform (such as less than 50% accuracy) by simply flipping their outputs. While this class does not include all possible fusers, it includes a wide class where the fuser is effective when at least some of the individual SPRTs are effective.

Theorem 4.1 *Consider the detection of a source with separable SPRT, and $\mathcal{M}_{\infty}(\mathcal{Z}_L, \epsilon_{D_Z}, \epsilon_{D_F}) > N$ and $\mathcal{M}_{\infty}(\mathcal{Z}_H, \epsilon_{F_Z}, \epsilon_{F_F}) > N$ for $\epsilon_{D_Z}, \epsilon_{D_F}, \epsilon_{F_Z}, \epsilon_{F_F}$ defined in Theorem 3.1. Let \mathcal{L}_M and \mathcal{L}_{F_+} denote majority and positive fusers based on SPRT decisions at individual sensors located at $(x_1, y_1), (x_2, y_2) \dots (x_N, y_N)$. Then for SPRT $\mathcal{L}_{\hat{\mathcal{S}}}$ based on δ -robust localization method, for sufficiently large n and N , and $\mathcal{L} = \mathcal{L}_M, \mathcal{L}_{F_+}$ we have:*

(i) *detection rates satisfy*

$$\begin{aligned} \mathcal{E}_D(\mathcal{L}_{\hat{\mathcal{S}}}) &> \\ [\mathcal{E}_D(\mathcal{L}) + (\mathcal{M}_{\infty}(\mathcal{Z}_L, \epsilon_{D_Z}, \epsilon_{D_F}) - N)] \delta(\epsilon_{D_Z}, n, N); \end{aligned}$$

(ii) *false alarm rates satisfy*

$$\begin{aligned} \mathcal{E}_F(\mathcal{L}_{\hat{\mathcal{S}}}) &< \\ [\mathcal{E}_F(\mathcal{L}) - (\mathcal{M}_{\infty}(\mathcal{Z}_H, \epsilon_{F_Z}, \epsilon_{F_F}) - N)] \delta(\epsilon_{F_Z}, n, N) \end{aligned}$$

Proof: The proof outline is similar to Theorem 3.1 and we present only the main points. For the majority fuser \mathcal{L}_M a direct application of the proof method in Theorem 3.1 shows that it makes a correct detection on at most N spherical cells. Similarly, any positive fuser F_+ corresponding to \mathcal{L}_{F_+} makes a correct detection on at most N spherical cells, but will make an error on other cells that constitute the packing number, hence the above bound is satisfied. \square

Compared to $\mathcal{L}_{\tau_L, \tau_H}$, the performance improvements of $\mathcal{L}_{\hat{\mathcal{S}}}$ over \mathcal{L}_M or \mathcal{L}_{F_+} require a larger packing number. Intuitively, such stronger requirement is expected since the fusers in general perform better than single sensors. The performances of $\mathcal{L}_{\tau_L, \tau_H}$, \mathcal{L}_M , \mathcal{L}_{F_+} , and $\mathcal{L}_{\hat{\mathcal{S}}}$ represent different cyber-physical trade-offs. Single-sensor detector represents lowest cyber cost but achieves the lowest performance, where as $\mathcal{L}_{\hat{\mathcal{S}}}$ achieves the highest performance with highest cyber cost. Both \mathcal{L}_M and \mathcal{L}_{F_+} represent intermediate points in terms of cyber cost and performance trade-offs.

5 Source Detection

In this section consider that source gives rise to the intensity $A_i = A_S/d_i^2$ at sensor location (x_i, y_i) , where $d_i = d((x_S, y_S), M_i)$. Sensor measurement $m_{i,j}$ observed at M_i at time j is distributed according to Poisson distribution in the first case and Gaussian distri-

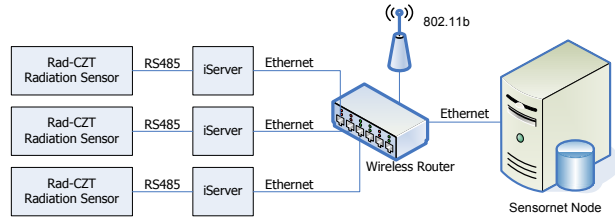


Figure 1: Equipment setup in the radiation test-bed.

bution in the second case. In either case, the measurements are assumed to be statistically independent across the sensors and time.

5.1 Radiation Source

The radiation count $m_{i,j}$ observed at M_i at time j is a Poisson random variable with parameter $\lambda = B_i = B(x_i, y_i)$ when there is no source present, and with $\lambda = A_i + B_i$, when source is present [10]. The likelihood function in this case is:

$$L(m_{i,1}, m_{i,2}, \dots, m_{i,n} | H_C) = \prod_{j=1}^{n_i} \frac{C^{m_{i,j}} e^{-C}}{m_{i,j}!}$$

where $C \in \{B_i, A_i + B_i\}$. The SPRT for detecting a radiation source can be expressed in terms of the sum of measurements as:

$$\frac{\ln \left[\frac{P_{0,1}}{1-P_{1,0}} \right] + nA_i}{\ln \left[\frac{A_i+B_i}{B_i} \right]} \leq \sum_{j=1}^n m_{i,j} \leq \frac{\ln \left[\frac{1-P_{0,1}}{P_{1,0}} \right] + nA_i}{\ln \left[\frac{A_i+B_i}{B_i} \right]}$$

which shows that it is separable. Note here that the computation of the thresholds requires the knowledge of source strength A_i .

There are several localization algorithms proposed for radiation sources, including adapting Gaussian model in [7], geometric method called the Difference Time Of Arrival (DTOA) method [19, 16, 25], mean of estimates method [17], and iterative pruning method [4]. The DTOA method to estimate (\hat{x}_u, \hat{y}_u) is shown to be δ -robust in (x, y) -space [19, 17].

5.1.1 Simulation Results

In our simulations, radiation sources are located uniformly inside $[0, 1000] \times [0, 1000]$ spatial grid with A chosen from $[1, 10^{12}]$ with $B(x,y) = 10$. The simulation programs have been implemented in C using random number generators from Numerical Recipes [12] and executed on a Redhat Linux workstation with a 2.8 GHz Intel processor. We randomly generated 10 sensor locations and executed both the Boolean fuser with fusion threshold computed using source strengths $f = 0.90, 0.91, \dots, 1.8$ times the background measurements at the local sensor with $P_{1,0} = P_{0,1} = 0.1$. We also computed the localization-based detection using the exact location of the source at the sensor located nearest to the source, which simulates perfect localization. Based on 100 measurements, the Boolean fuser

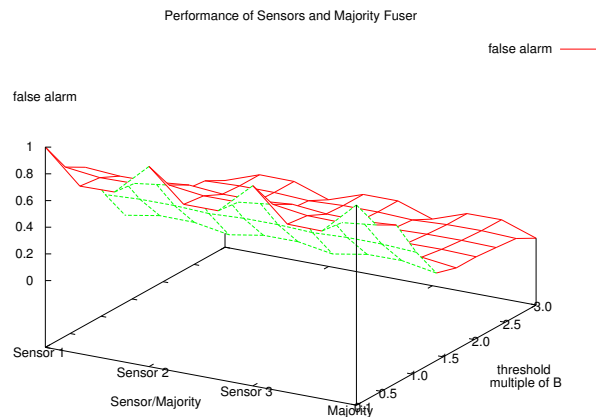


Figure 2: False alarm rate for different thresholds [18].

generated false alarm for $f \leq 0.92$, and missed detections for $f \geq 1.1$ and $f \geq 1.4$ corresponding to medium and high source strengths, respectively; here, the measured ratios of source to background strengths for medium and high sources are in the ranges $[1.1, 4.1]$ and $[2.0, 13]$, respectively. Thus Boolean fuser leads to successful detection only if the threshold are computed with f in the range $(0.92, 1.1)$ and $(0.92, 1.4)$ for medium and high source strengths, respectively. The localization-based detector correctly detected the source with no false alarms in both cases without requiring the knowledge of the source strength.

We discuss next the performance details for the specific case in which sensors M_1 and M_2 are located at $(0, 0)$ and $(0, 1000)$ on the grid and M_3 is such that $y_3 = 1000$ and x_3 is uniformly chosen from $[0, 1000]$. We first consider the case of background only, that is no source is present. The false alarms rate is plotted for each sensor and majority fuser as a function of threshold, which is varied from $B/10$ to $3B$ in steps of $B/10$, as shown in Figure 2. For all sensors and majority fuser, the false alarm rate is 100% when threshold is at or below $1.1B$, and zero above that, for all $P_{0,1} = P_{1,0}$ values of 0.1, 0.01 and 0.001.

We now consider that a source of strength $A_S = 10^6$ is present, which generates an average radiation level of 1.17 times over the background level of $B(x,y) = 10$, as shown in row 3 of Table 2. To avoid high false alarm, the threshold τ_H must be chosen above $1.1B(x,y)$. But for thresholds $\tau_H = 1.5B(x,y)$ and higher only one sensor was able to detect the source; thus while there are no false alarms the target is completely missed. These examples illustrate the challenge of picking suitable threshold values for the detectors. On the other hand, DTOA method correctly concluded the detection in this case with 26, 100, 133 measurements for $P_{0,1} = P_{1,0}$ values of 0.1, 0.01 and 0.001, respectively.

ave rad level at M_1	M_1 det (%)	majority det (%)	DTOA det (%)
1.02 $B_{(x,y)}$	1	0	65
1.09 $B_{(x,y)}$	16	10	100
1.17 $B_{(x,y)}$	51	96	100
2.09 $B_{(x,y)}$	99	100	100
2.84 $B_{(x,y)}$	99	100	100
100.0 $B_{(x,y)}$	100	100	100

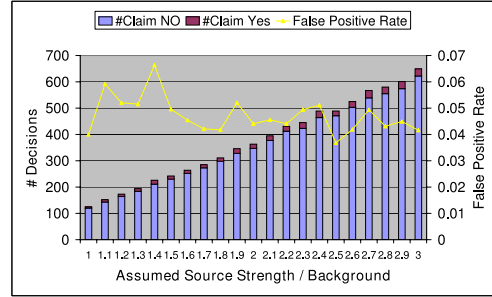
Table 1: Summary of simulation results [18].

Based on 100 randomly generated sources for different source strengths, we show the detection rates of M_1 , majority fuser for threshold $\tau_H = 1.1B_{(x,y)}$, and DTOA method in columns 2, 3 and 4 of Table 2, respectively, for $P_{0,1} = P_{1,0} = 0.01$. The threshold is about 10% higher than the average background level, which is suggested in [11]. While this threshold achieved zero false alarm rate, its detection rate depends on the source strength. For source strengths that lead to about 17% increase in the average radiation levels, M_1 was only about 51% accurate although the majority fuser achieved 96% detection. DTOA method achieved 100% detection when average increase in radiation at M_1 was at least 9% or higher above the background level.

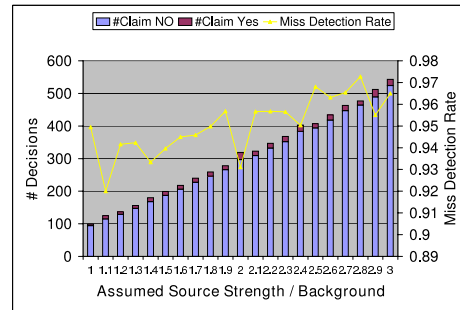
These results illustrate the main idea behind Theorems 3.1 and 4.1: fixing the threshold values makes the SPRT effective within certain region of source strengths, but makes it ineffective elsewhere. On the other hand, DTOA dynamically estimates the parameters, and uses the source and background distributions to compute the thresholds. Fixed-threshold SPRT is effective in only one such region, whereas DTOA is effective in all of them, and their number is characterized by the packing number of the state-space.

5.1.2 Testbed Results

Three radiation detection test-beds are set up at Oak Ridge National Laboratory, Purdue University, University of Illinois at Urbana-Champaign, all with the same configuration shown in Figure 1. A Cs-137 radiation source of strength 0.95 μ -Curies is used on a table top with RFTrax RAD-CZT sensors to collect measurements. For the testbed measurements we tested SPRT with τ_H ranging from \hat{B} to $3\hat{B}$, where \hat{B} is the estimate of average background radiation level at M_1 . In Figure 3(a), we show false alarm rate which is about 6% for $\tau_H \leq 1.4\hat{B}$ and drops off to 4% for higher values. But when source is present, the detection rate is below 94% for $\tau_H \leq 1.4\hat{B}$, and 97% detection rate is achieved only for $\tau_H \geq 2.7\hat{B}$. For example, the choice $\tau_H = 1.7\hat{B}$ achieves about 95% detection rate with 4% false alarm rate, which was the lowest for any choice.



(a) background



(b) source present

Figure 3: Testbed results for different thresholds [18].

5.2 Gaussian Source

We now consider that the measurement $m_{i,j}$ observed at M_i at time j is a normally distributed with mean $\mu = B_i = B_{(x_i,y_i)}$ when there is no source present, and with $\mu = A_i + B_i$, when source is present [26, 24]. The likelihood function in this case is:

$$L(m_{i,1}, m_{i,2}, \dots, m_{i,n} | H_C) = \prod_{j=1}^{n_i} \frac{1}{2\pi\sigma} \exp\left(-\frac{(m_{i,j} - C)^2}{\sigma^2}\right)$$

where $C \in \{B_i, A_i + B_i\}$. The SPRT for detecting this source against the background can be expressed in terms of the sum of measurements as:

$$\begin{aligned} & \frac{1}{2A_i} \left[n(A_i^2 + 2A_iB_i) - \ln\left(\frac{\sigma^2(1 - P_{0,1})}{P_{1,0}}\right) \right] \\ & \leq \sum_{j=1}^n m_{i,j} \\ & \leq \frac{1}{2\sigma} \left[n(A_i^2 + 2A_iB_i) - \ln\left(\frac{\sigma^2 P_{0,1}}{(1 - P_{1,0})}\right) \right] \end{aligned}$$

which establishes the separability property needed for applying Theorems 3.1 and 4.1 that lead to effective localization-based detection.

6 Conclusions

We considered the detection problem of a source with scalar intensity inside a two-dimensional monitoring area using random sensor measurements in presence of a background process. We proposed a detection method that utilizes a robust localization method followed by an adaptive SPRT. Under smoothness and non-smoothness conditions on the probability ratios

and packing conditions on state-space, we showed that this method provides better performance compared to SPRT-based single sensor detectors, and also their majority and certain other fusers. More extensive simulations and experiments would help gain further understanding of the localization-based detection approach. It would be of future interest to investigate the number of measurements needed by SPRT at sensors and fuser to reach a decision. Also, it would be of future interest to investigate SPRT detectors with multiple thresholds that can cover several spherical cells of the state-space.

Acknowledgments

This work is funded by the Mathematics of Complex, Distributed, Interconnected Systems Program, Office of Advanced Computing Research, U.S. Department of Energy, and also by the SensorNet Program, Office of Naval Research, and was performed at Oak Ridge National Laboratory managed by UT-Battelle, LLC for U.S. Department of Energy under Contract No. DE-AC05-00OR22725.

References

- [1] M. Anthony and P. L. Bartlett. *Neural Network Learning: Theoretical Foundations*. Cambridge University Press, 1999.
- [2] D. E. Archer, B. R. Beauchamp, G. J. Mauger, K. E. Nelson, M. B. Mercer, D. C. Pletcher, V. J. Riot, J. L. Schek, and D. A. Knapp. Adaptable radiation monitoring system and method, 2006. U.S. Patent 7,064,336 B2.
- [3] S. M. Brennan, A. M. Mielke, and D. C. Torney. Radiation detection with distributed sensor networks. *IEEE Computer*, pages 57–59, August 2004.
- [4] J. C. Chin, C. Y. T. Ma, D. K. Y. Yau, N. S. V. Rao, M. Shankar, and Y. Yang. Accurate localization of low-level radioactive source under noise and measurement errors. In *The 6th ACM Conference on Embedded Networked Sensor Systems: Sensys*, 2008.
- [5] C. K. Chow. Statistical independence and threshold functions. *IEEE Trans. Electronic Computers*, EC-16:66–68, 1965.
- [6] P. E. Felau. Comparing a recursive digital filter with the moving-average and sequential probability-ratio detection methods for SNM portal monitors. *IEEE Transactions on Nuclear Science*, 40(2):143–146, 1993.
- [7] A. Gunatilaka, B. Ristic, and R. Gailis. On localisation of a radiological point source. In *International Conference on Information, Decision and Control*. 2007.
- [8] K. D. Jarman, L. E. Smith, and D. K. Carlson. Sequential probability ratio test for long-term radiation monitoring. *IEEE Transactions on Nuclear Science*, 51(4):1662–1666, 2004.
- [9] N. L. Johnson. Sequential analysis: A survey. *Journal of Royal Statistical Society, Series A*, 124(3):372–411, 1961.
- [10] G. F. Knoll. *Radiation Detection and Measurement*. John Wiley, 2000.
- [11] K. E. Nelson, J. D. Valentine, and B. R. Beauchamp. Radiation detection method and system using the sequential probability ratio test, 2007. U.S. Patent 7,244,930 B2.
- [12] W. H. Press, S. A. Teukolsky, W. T. Vetterling, and B. P. Flannery. *Numerical Recipes in C*. Cambridge University Press, 1992.
- [13] N. S. V. Rao. Measurement-based statistical fusion methods for distributed sensor networks. In S. S. Iyengar and R. R. Brooks, editors, *Distributed Sensor Networks*. Chapman and Hall/CRC Publishers, 2005.
- [14] N. S. V. Rao, J. C. Chin, D. K. Y. Yau, C. Y. T. Ma, and R. N. Madan. Cyber-physical trade-offs in distributed detection networks, 2010. manuscript.
- [15] N. S. V. Rao and V. Protopopescu. Function estimation by feedforward sigmoidal networks with bounded weights. *Neural Processing Letters*, 7:125–131, 1998.
- [16] N. S. V. Rao, M. Shankar, J. C. Chin, D. K. Y. Yau, S. Srivathsan, S. S. Iyengar, Y. Yang, and J. C. Hou. Identification of low-level point radiation sources using a sensor network. In *International Conference on Information Processing in Sensor Networks*, 2008.
- [17] N. S. V. Rao, M. Shankar, J. C. Chin, D. K. Y. Yau, Y. Yang, J. C. Hou, X. Xu, and S. Sahni. Localization under random measurements with applications to radiation sources. In *International Conference on Information Fusion*, 2008.
- [18] N. S. V. Rao, M. Shankar, J. C. Chin, D. K. Y. Yau, Y. Yang, X. Xu, and S. Sahni. Improved SPRT detection using localization with application to radiation sources. In *International Conference on Information Fusion*, 2009.
- [19] N. S. V. Rao, X. Xu, and S. Sahni. A computational geometric method for dtoa triangulation. In *International Conference on Information Fusion*, 2007.
- [20] A. Sundaresan, P. K. Varshney, and N. S. V. Rao. Distributed detection of a nuclear radioactive source using fusion of correlated decisions. In *International Conference on Information Fusion*, 2007.
- [21] H. L. Van Trees. *Detection, Estimation and Modulation Theory, Part I*. John Wiley, 1968.
- [22] P. K. Varshney. *Distributed Detection and Data Fusion*. Springer-Verlag, 1997.
- [23] G. B. Wetherill. *Sequential Methods in Statistics*. Methuen and Co., 1966.
- [24] G. Xing, R. Tan, B. Liu, J. Wang, X. Jia, and C. Yi. Data fusion improves the coverage of wireless sensor networks. In *Proceedings of Mobicom*, 2009.
- [25] X. Xu, N. S. V. Rao, and S. Sahni. A computational geometry method for localization using difference of distances. *ACM Transactions on Sensor Networks*, 2010. in press.
- [26] M. Zhu, S. Ding, R. R. Brooks, Q. Wu, S. S. Iyengar, and N. S. V. Rao. Fusion of threshold rules for target detection in wireless sensor networks. *ACM Transactions on Sensor Networks*, 2010.